European Journal of Immunology

TCR-engineered T cells: A model of inducible TCR expression to dissect the interrelationship between two TCRs

Simone Reuß[1], Zsolt Sebestyén[2], Niels Heinz[3], Rainer Loew[4], Christopher Baum[3], Reno Debets[2] and Wolfgang Uckert[1,5]

[1] Max-Delbrück-Center for Molecular Medicine, Berlin, Germany
[2] Experimental Tumor Immunology, Department of Medical Oncology, Erasmus University Medical Center — Daniel den Hoed Cancer Center, Rotterdam, The Netherlands
[3] Experimental Hematology, Hannover Medical School, Hannover, Germany
[4] Eufets GmbH, Idar-Oberstein, Germany
[5] Institute of Biology, Humboldt University of Berlin, Berlin, Germany

TCR gene modified T cells for adoptive therapy simultaneously express the Tg TCR and the endogenous TCR, which might lead to mispaired TCRs with harmful unknown specificity and to a reduced function of TCR-Tg T cells. We generated dual TCR T cells in two settings in which either TCR was constitutively expressed by a retroviral promoter while the second TCR expression was regulable by a Tet-on system. Constitutively expressed TCR molecules were reduced on the cell surface depending on the induced TCR expression leading to strongly hampered function. Besides that, using fluorescence resonance energy transfer we detected mispaired TCR dimers and different pairing behaviors of individual TCR chains with a mutual influence on TCR chain expression. The loss of function and mispairing could not be avoided by changing the TCR expression level or by introduction of an additional cysteine bridge. However, in polyclonal T cells, optimized TCR formats (cysteineization, codon optimization) enhanced correct pairing and function. We conclude from our data that (i) the level of mispairing depends on the individual TCRs and is not reduced by increasing the level of one TCR, and (ii) modifications (cysteineization, codon optimization) improve correct pairing but do not completely exclude mispairing (cysteineization).

Keywords: Fluorescence resonance energy transfer (FRET) · Inducible gene expression · TCR gene optimization · TCR gene therapy · TCR mispairing

Additional supporting information may be found in the online version of this article at the publisher's web-site

Introduction

The adoptive transfer of TCR gene-modified T cells showed first clinical success in the treatment of melanoma and synovial sarcoma [1, 2]. But also detrimental effects of TCR gene therapy became obvious as on-target toxicity was observed in two clinical trials due to tumor-associated Ag expression on healthy tissue [3, 4]. In addition, off-target side effects can potentially occur due to TCR gene transfer that creates dual TCR T cells with mispaired TCR dimers harboring the risk to recognize self-antigens. Although in patients treated by TCR gene therapy such toxicity was not reported so far, lethal autoimmune pathology due to mispaired

Correspondence: Dr. Wolfgang Uckert
e-mail: wuckert@mdc-berlin.de

TCR dimers was seen in a mouse model in which animals received TCR-Tg T cells using a protocol mimicking clinical application [5]. The application of T-cell populations with unique TCR specificity (e.g. virus-specific T-cell clones) may limit the formation of mispaired TCR dimers. However, also in this setting, mispaired TCRs were formed with potentially hazardous specificities recognizing both allo- and auto-Ags in a HLA class I and II restricted fashion [6].

Therefore, efforts have been made to diminish the occurrence of mispaired TCR dimers. First, the stoichiometric expression of the TCRα and TCRβ chain genes can be improved by using a viral peptide linker instead of an internal ribosomal entry site in the transgene cassette [7–9]. Second, numerous modifications of the TCR gene sequence were performed to reduce the formation of mispaired TCRs [10–16]; reviewed in [17]. Two of the most often utilized modifications are the replacement of the human TCR constant (C-) regions by the mouse counterparts (murinization) [12, 18, 19] and the insertion of a second cysteine bridge (cysteineization) into the TCR C-region [13, 14]. Especially, cysteineization reduced the incidence of autoimmunity in a mouse model [5] and the appearance of neoreactivities in vitro [6]. A more general approach is the codon optimization of the TCR genes that improves the expression of most if not all Tg TCRs and thereby limits those of the endogenous ones [7].

Little is known about the quantitative relationship between endogenous and transferred TCRs with respect to surface expression of individual TCR chains, function, and pairing. We generated dual TCR-expressing T cells by gene transfer of two model TCRs into mouse 58 T cells harboring no endogenous TCR molecules or by transfer of one TCR into WT T cells to study surface expression, function, and pairing of unmodified or modified TCRs (cysteineization, codon optimization). To analyze pairing, we utilized fluorescence resonance energy transfer (FRET) — a method that allows the determination of the regional proximity of two molecules by labeling with suitable fluorophores.

Results

TCR expression is inducible by a Tet-regulated retrovirus SIN vector

The P14 TCR, specific for the glycoprotein (gp33) of the lymphocytic choriomeningitis virus, and the OVA-specific OT-I TCR were expressed by a doxycycline (Dox, Tet)-regulated gammaretrovirus SIN vector [20] in 58 cells [21], which do not express an endogenous TCR. By adding Dox concentrations from 0.01 to 1.0 μg/mL for 24 h, TCR expression was achieved in T-cell clones ($P14^{ind}$ and $OT\text{-}I^{ind}$) measured by flow cytometry (Fig. 1A–D). We determined the kinetics of inducibility and measured already 4 h after addition of 1 μg/mL Dox P14 and OT-I TCR expression that reached its maximum at 16 h and remained stable until 24 h. After deprivation of Dox, expression of both TCRs decreased within 24 h and was no longer detectable after 72 h (Fig. 1E). For analysis of Tet-regulated TCR-mediated functionality, TCR^{ind} T-cell clones were co-cultured with splenocytes loaded with cognate peptide. $OT\text{-}I^{ind}$

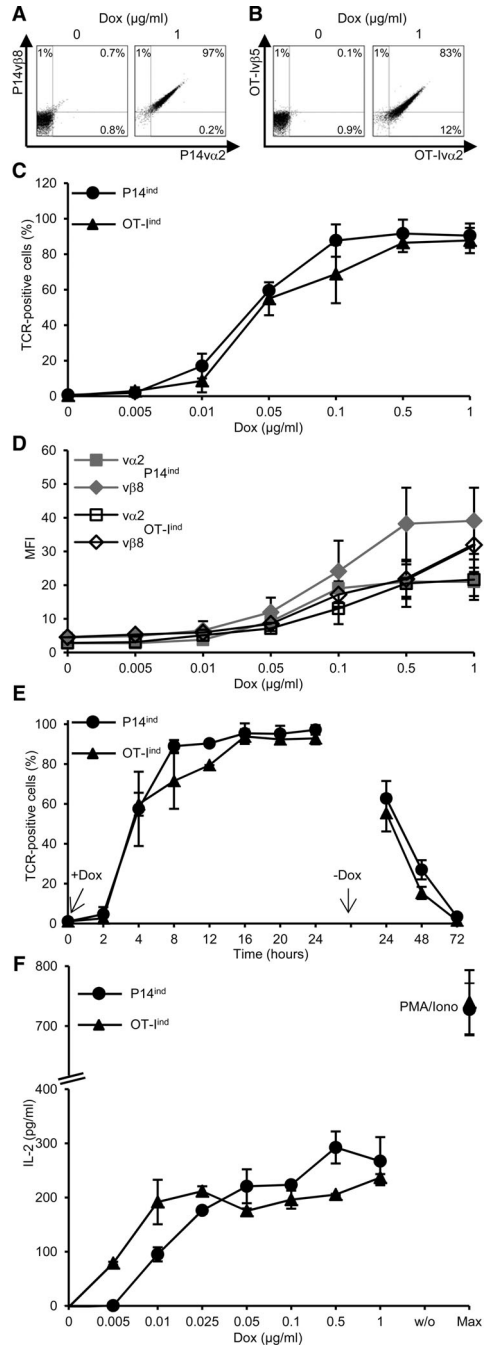

Figure 1. Inducible TCR expression in single TCR-Tg T cells. T-cell clones expressing $P14^{ind}$ or $OT\text{-}I^{ind}$ TCR were seeded at a density of 4×10^5/mL and incubated for 24 h with different concentrations of Dox. TCR expression was analyzed by flow cytometry and living cells discriminated in FSC/SSC dot plot. Dot plot of (A) $P14^{ind}$ or (B) $OT\text{-}I^{ind}$ living cells stained for TCR chains. (C) Percentages or (D) MFI of TCRvα and TCRvβ chain double-positive cells as a function of Dox concentration. (E) Percentage of TCR-positive cells as a function of incubation time in presence of Dox (1 μg/mL). (C–E) Data are shown as mean ± SD ($n = 3$–6) and are pooled from at least three independent experiments. (F) Co-cultivation of Dox-induced TCR-expressing 58 T cells with irradiated C57BL/6 splenocytes loaded with 10 μM peptide ($gp_{33–41}$ for P14 TCR and $OVA_{257–264}$ for OT-I TCR). As a control no peptide (w/o) or an unspecific stimulus with PMA and ionomycin (max) was added. IL-2 amount was determined by ELISA. Bars indicate mean of duplicates and mean deviation. One representative experiment of two is shown.

T cells already secreted IL-2 when TCR expression was induced with 0.005 μg/mL Dox (Fig. 1F), although at this concentration almost no TCR expression was observed (Fig. 1C). Addition of Dox between 0.01 and 1.0 μg/mL yielded similar amounts of IL-2. IL-2 secretion of $P14^{ind}$ T cells was detectable after addition of 0.01 μg/mL Dox and increased with higher Dox concentrations (Fig. 1F).

These data indicate that using the Tet-regulated vector we achieved different TCR expression levels and TCR function depending on the Dox concentration.

Gain of function of one TCR is accompanied by loss of function of the second TCR

To analyze the interrelationship of two TCRs, we generated dual TCR-Tg 58 T cells in which one TCR was expressed under the control of the constitutive promoter of the retroviral vector LXSN, while the expression of the second TCR was Dox-inducible (Fig. 2A).

In the first setting, the OT-I TCR was constitutively expressed in 58 T cells and the P14 TCR expression was induced ($OT\text{-}I^{con}/P14^{ind}$; where con is constitutive expression and ind is induced expression) using different Dox concentrations (no Dox – "off," 0.05 μg/mL – "med," 1.0 μg/mL – "high"). P14 TCR expression increased as a function of Dox concentration from 71% (med) to 96% (high) (Fig. 2B). The increasing percentage of P14 TCR molecules on the cell surface did not influence the percentage of the cells constitutively expressing OT-I TCR since this was 98% at med and high Dox concentrations. However, the number of TCR molecules per cell as measured by MFI decreased for the OT-Iνα2 chain from 51 (off) to 30 (high) (by 41%) and for the OT-Iνβ5 chain from 17 (off) to 13 (high) (by 24%). TCR molecules on the cell surface were quantified more precisely with secondary FITC Ab and with the help of calibrated FITC-labeled beads. This method revealed a decrease of 49 ± 29% for OT-Iνα2 chain and 57 ± 7% for the OT-Iνβ5 chain (Fig. 2C).

In parallel to the decrease of OT-I TCR molecules, we observed a gradual decrease in its function as measured by IL-2 release after co-cultivation with OVA peptide-loaded splenocytes whereas the induced P14 TCR gained function (Fig. 2D).

In the second setting, the P14 TCR was constitutively expressed, while the expression of the OT-I TCR was induced ($P14^{con}/OT\text{-}I^{ind}$). Here, the OT-I TCR expression increased depending on Dox concentration from 68% (med) to 87% (high). In parallel, the expression of the P14 TCR slightly decreased from 99 to 93% (Fig. 2F) as well as the MFI of P14vα2 chain from 71 (off) to 23 (high) (by 68%) and of P14vβ8 chain from 23 (off) to 13 (high) (by 44%). The quantification confirmed the decrease of TCR molecules, namely 63 ± 18% for P14vα2 and 39 ± 13% for P14vβ8 (Fig. 2G). The reduced expression of the P14 TCR was accompanied by a complete loss of its function, while the induced OT-I TCR expression resulted in a gain of function (Fig. 2H).

Although dual TCR T cells appear to present both TCRs, the reduction of TCR molecules by ~50% on the cell surface is sufficient to reduce or completely shut down IL-2 secretion after TCR trigger depending on the influence of the second TCR.

Formation of mispaired TCR dimers contributes to the diminished TCR function

Beside reduced levels of TCR molecules on the cell surface, we assumed that mispairing of TCR chains contributed to the loss of function of the TCR^{con}. FRET measurements for the detection of the occurrence of mispaired TCR dimers were performed. In $OT\text{-}I^{con}/P14^{ind}$ 58 T cells, the FRET efficiency of the constitutively expressed OT-I TCR stayed at a similar level (33.7 ± 5% no Dox vs. 32.5 ± 8% high Dox) even when P14 TCR expression was induced in 85.9 ± 9% TCR-positive cells (Fig. 2E). The induced P14 TCR did not have a significant lower FRET efficiency of 23.3 ± 8% with high Dox concentration compared to the OT-I TCR, which was similar to the FRET efficiency of OT-Iνα2/P14vβ8 (22.6 ± 8%). The mispaired TCR dimer P14vα2/OT-Iνβ5 showed a significant lower FRET efficiency of 12 ± 7% compared to OT-I and P14 TCR. These data show that there is a considerable degree of OT-I and P14 TCR mispairing with a preference for the occurrence of OT-Iνα2/P14vβ8 dimers. The FRET efficiency of the OT-I TCR that stayed stable with Dox is reflected by the occurrence of equal amounts of corresponding TCR chains. Quantification of TCR chains showed a similar decrease or increase of $OT\text{-}I^{con}$ or $P14^{ind}$ molecules, respectively, for OT-Iνα2 from 1830 ± 480 to 940 ± 360; OT-Iνβ5 from 1910 ± 210 to 820 ± 130 and for P14vα2: 1670 ± 460; P14vβ8: 1850 ± 560 with 1 μg/mL Dox (Fig. 2C). Nevertheless, this did not exclude the occurrence of mispaired TCR dimers.

In $P14^{con}/OT\text{-}I^{ind}$ 58 T cells, the FRET efficiency measured for P14 TCR significantly decreased from 35 ± 3 to 19 ± 6% when the OT-I TCR was induced with high Dox concentration (76.4 ± 17% TCR-positive cells) (Fig. 2I). The FRET efficiency of correct OT-I TCR pairing was 25 ± 6%. Again, a preference was noted for the mispaired TCR dimer comprising of OT-Iνα2/P14vβ8 (21 ± 8%) and not P14vα2/OT-Iνβ5 (12 ± 3%). The reduced FRET efficiency of the P14 TCR with Dox was also confirmed by the unequal decrease of the corresponding TCR chain molecules (P14vα2 from 4360 ± 1080 to 1600 ± 780; P14vβ8 from 3200 ± 440 to 1970 ± 400) and the unequal induction of OT-I TCR with Dox (OT-Iνα2: 1280 ± 680 and OT-Iνβ5: 830 ± 50) (Fig. 2G). In sum, these cells harbored mispaired TCR dimers and a reduced capability of prober P14 TCR pairing.

Similar results were obtained in both models when med Dox concentrations were applied (data not shown). Tetramer staining to dissect proper TCR formation was not possible with the 58 T-cell line due to unspecific binding of tetramer to the transferred CD8α molecule that was needed for the functional analysis of the TCRs. Unspecific tetramer binding could not be blocked by CD8α antibody.

In summary, FRET analysis of both TCR combinations indicated that the TCR dimer OT-Iνα2/P14vβ8 occurred to a similar level as the correctly paired P14 and OT-I TCR. Thus, the detected mispaired TCRs as well as the reduced TCR molecules on the cell

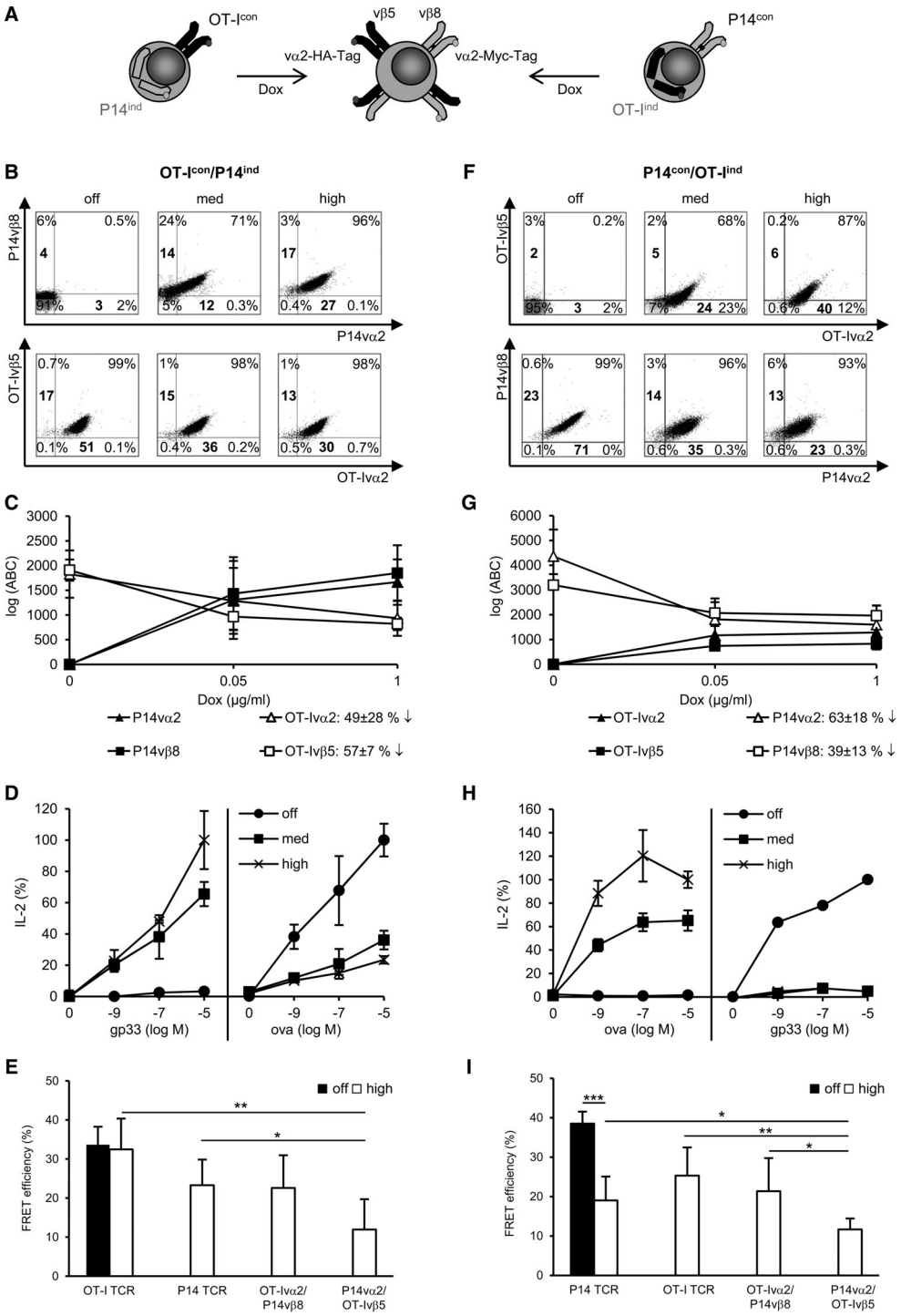

Figure 2. Analysis of TCR expression, functionality, and TCR mispairing in dual TCR T cells. (A) Schematic picture of the generation of dual TCR T cells. Fifty-eight T cells (4×10^5/mL) were incubated for 24 h with 1 µg/mL (high), 0.05 µg/mL (med), or without (off) Dox. Dot plots of cells stained for (B) constitutively expressed OT-I TCR and induced P14 TCR (OT-I^{con}/$P14^{ind}$) or for (F) constitutively expressed P14 TCR and induced OT-I TCR ($P14^{con}$/OT-I^{ind}). (B, F) Bold numbers indicate MFI. Quantification of TCR chains in (C) OT-I^{con}/$P14^{ind}$ cells and (G) $P14^{con}$/OT-I^{ind} cells. Antibody binding capacity (ABC) represents molecules on cell surface. (C, G) Data are shown as mean ± SD ($n = 3$) and are pooled from three independent experiments. IL-2 secretion as a function of constitutive and induced TCR expression in (D) OT-I^{con}/$P14^{ind}$ cells and (H) $P14^{con}$/OT-I^{ind} cells after 24 h co-cultivation with gp33/OVA peptide-loaded splenocytes. IL-2 amount, measured by ELISA, is given as percentage of the maximal secretion, which was determined for TCR^{ind} at 10 µM cognate peptide and high Dox ($P14^{ind}$: 63 pg/mL; OT-I^{ind}: 141 pg/mL) and for TCR^{con} at 10 µM cognate peptide and without Dox (OT-I^{con}: 82 pg/mL; $P14^{con}$: 103 pg/mL). Data points indicate mean of duplicates and mean deviation. For B, D, F, H one representative experiment of three or more is shown. FRET analysis of correctly and mispaired TCRs on dual TCR (E) OT-I^{con}/$P14^{ind}$ cells and (I) $P14^{con}$/OT-I^{ind} cells. (E, I) Data are shown as mean + SD ($n = 3$–5) and are pooled from at least three independent experiments. $^*p < 0.05$, $^{**}p < 0.01$, $^{***}p < 0.001$; unpaired Student's *t*-test.

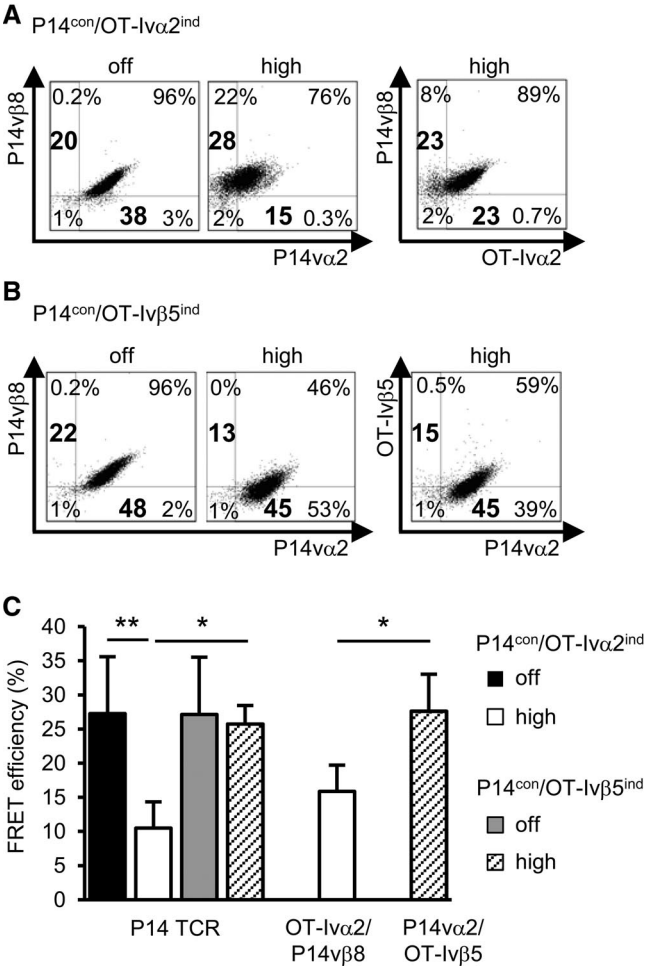

Figure 3. Induction of single OT-I TCR chains in dual 58 T cells. T cells (4×10^5/mL) were incubated for 24 h with 1 μg/mL (high) or without (off) Dox. TCR chain staining of P14 and (A) P14vβ8/OT-Ivα2 ($P14^{con}$/OT-Iva2^{ind}) or (B) P14vα2/OT-Ivβ5 ($P14^{con}$/OT-Ivb5^{ind}) is shown as dot plots. One of three experiments is shown. Bold numbers indicate MFI. (C) FRET analysis of correctly and mispaired TCRs on $P14^{con}$/OT-Iva2^{ind} or vβ5^{ind} cells. Data are shown as mean ± SD ($n = 3$) and are pooled from three independent experiments. $^*p < 0.05$, $^{**}p < 0.01$; unpaired Student's *t*-test.

surface of the constitutively expressed TCR in both T-cell clones explain the reduction or even loss of function of either the OT-I or the P14 TCR. The different pairing behavior of TCR chains also influences the expression of the corresponding TCR chain on the cell surface, which was seen to be unequal in $P14^{con}$+OT-I^{ind} cells.

To further confirm the occurrence of mispaired TCRs, $P14^{con}$ T-cell clones with single inducible OT-I TCR chains were constructed. Induced OT-Iva2 TCR chain expression led to a decrease from 96 to 76% P14 TCR-positive cells ($P14^{con}$/OT-Iva2^{ind}), which was due to the partial loss of P14va2 TCR chain expression (MFI decreased by 61% from 38 to 15) (Fig. 3A). The induced OT-Iva2 paired with the P14vβ8 TCR chain (89%) and therefore, partially displaced the P14va2 chain. Induction of the OT-Ivβ5 TCR chain expression diminished P14 TCR-positive cells from 96 to 46% ($P14^{con}$/OT-Ivb5^{ind}) and formed with the P14va2 TCR chain 59% double-positive T cells thereby partially replacing the P14vβ8 chain (MFI decreased by 41% from 22 to 13) (Fig. 3B). FRET efficiency of the endogenous P14 TCR was significantly reduced when the OT-Iva2 TCR chain was induced (27 ± 8 vs. 10 ± 4%), but not when the OT-Ivβ5 TCR chain was induced (27 ± 8 vs. 26 ± 3%) (Fig. 3C). The mispairing of the OT-Iva2 with the P14vβ8 chain showed a FRET efficiency of 16 ± 4%, which was significantly lower as the mispairing of the P14va2 chain with the OT-Ivβ5 chain (28 ± 5%). These results demonstrate that both inducible single OT-I TCR chains can partially replace their P14 TCR chain counterparts, but that the inducible OT-Iva2 chain reduces pairing of the P14 TCR by pairing with the P14vβ8 chain more easily, whereas the OT-Ivβ5 chain showed an equal pairing efficiency to the P14va2 as P14vβ8. These data confirmed the differential pairing behavior of individual TCR chains.

A second cysteine bridge in P14 TCR does not prevent the formation of mispaired TCR dimers

Since proper P14 TCR chain pairing was strongly impaired by the induced OT-I TCR, we modified the P14 TCR by cysteineization [13, 14] and generated two T-cell clones expressing P14cys and OT-I^{ind} TCRs ($P14cys^{con}$+OT-I^{ind}). Induction of OT-I TCR expression in cl.9 ($P14cys^{con}$/OT-I^{ind} cl.9) (96%) decreased the percentage of P14cys TCR-positive cells from 96 to 68% (Fig. 4A). In parallel, we measured a complete loss of function of the P14cys TCR (Fig. 4B). In the second 58 T-cell clone ($P14cys^{con}$/OT-I^{ind} cl.7), moderate OT-I TCR expression was induced (57%) (Fig. 4D). Here, the induction of OT-I TCR expression did not diminish the percentage of P14 TCR-positive cells (97% vs. 96%) but again led to a complete loss of function of the P14cys TCR (Fig. 4E).

Independently of the strength of the OT-I TCR induction, TCR mispairing was detected by FRET similarly (Fig. 4C and F) as in the noncysteineized $P14^{con}$+OT-I^{ind} cells (Fig. 2I), but moderate induced OT-I TCR expression in cl.7 could not reduce P14 prober pairing as highly as induced OT-I TCR expression in cl.9.

Nevertheless, these data indicate that neither the expression level of the OT-I TCR nor the introduction of a cysteine modification into the P14 TCR C-region could rescue the function of the P14 TCR and prevent mispairing in this dual TCR T-cell model.

The combination of different TCR modifications improves P14 TCR chain pairing

So far, our results indicate that cysteineization of the P14 TCR did not prevent mispairing with OT-I TCR chains in a model T-cell line. To analyze these modified TCRs in a more clinically relevant situation, primary polyclonal T cells were transduced. Beside cysteineization, also codon optimization was included as TCR format [7]. In C57BL/6 primary mouse T cells, the expression level of WT and cysteineized TCR formats could be considerably increased by codon optimization (Fig. 5A). To analyze whether these

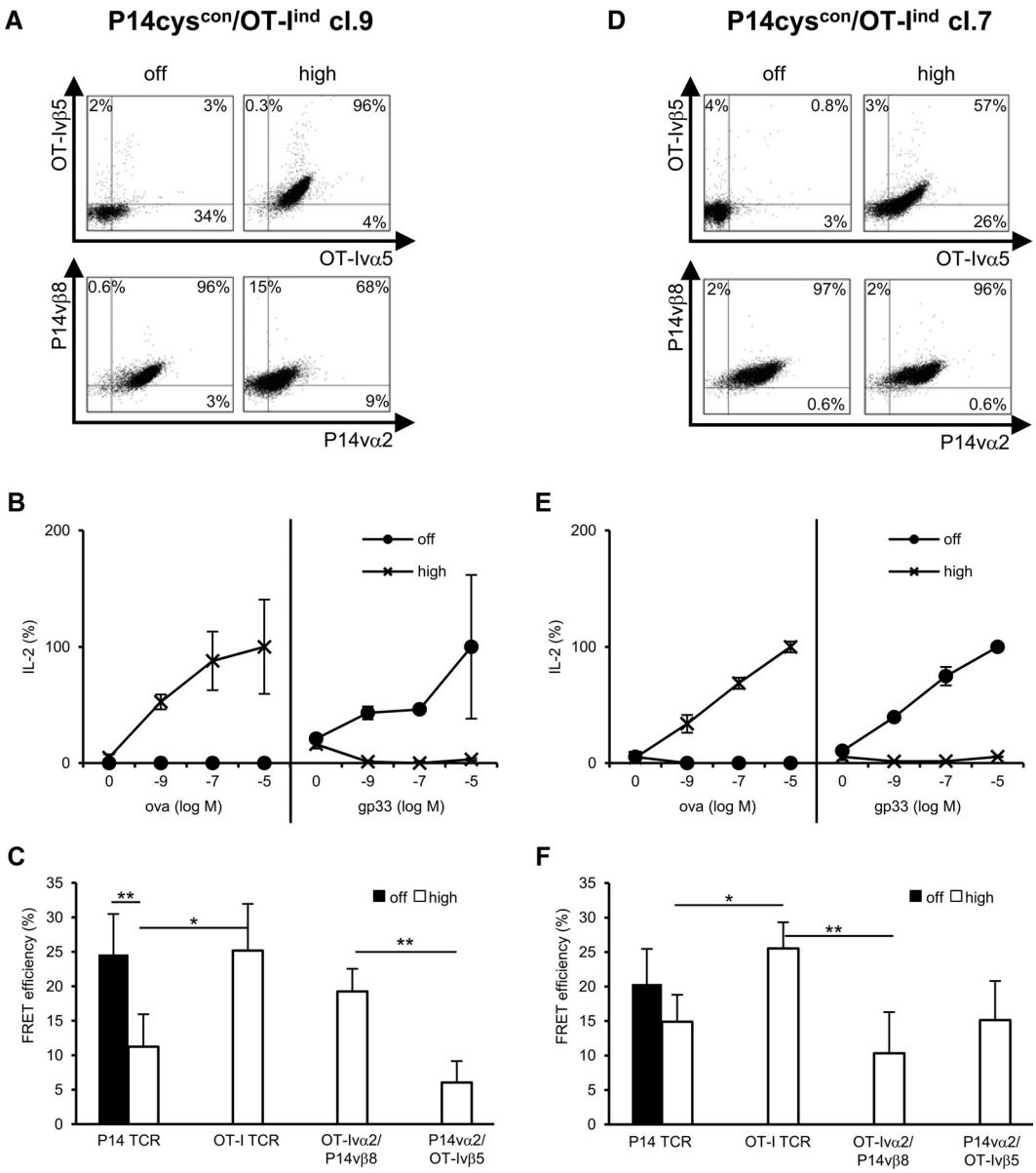

Figure 4. Cysteineization of P14 TCR in dual TCR T cells. Fifty-eight T cells (4×10^5/mL) were incubated for 24 h without (off) or with 1 μg/mL (high) Dox and stained for constitutive cysteine-modified P14 (P14cys) TCR and induced OT-I TCR expression, P14cys^{con}/OT-I^{ind} cl.9 (A) and cl.7 (D). IL-2 secretion in dual TCR 58 T cells as function of constitutive P14cys TCR and induced OT-I TCR expression, cl.9 (B) and cl.7 (E). IL-2 amount is given as percentage of the maximal secretion, which was determined for OT-I^{ind} at 10 μM OVA peptide and high Dox (cl.9: 257 pg/mL; cl.7: 321 pg/mL) and for P14cys^{con} at 10 μM gp33 peptide and without Dox (cl.9: 101 pg/mL; cl.7: 313 pg/mL). Data points indicate mean of duplicates and mean deviation. (A, B, D, E) One representative experiment of three is shown. FRET analysis of correctly and mispaired TCRs on dual TCR P14cys^{con}/OT-I^{ind} cl.9 (C) and cl.7 (F). (C, F) Data are shown as mean ± SD ($n = 3$) and are pooled from three independent experiments. $^*p < 0.05$, $^{**}p < 0.01$; unpaired Student's *t*-test.

differences also apply to TCR function, a co-cultivation of equilibrated numbers of TCR-Tg T cells with peptide-loaded splenocytes was performed. No difference in IFN-γ release was found for the different TCR formats at higher peptide concentrations (100 and 10 pM). However, at lower peptide concentrations (1 pM), the modified TCR formats, especially those of the OT-I TCR, showed a higher function in comparison to the WT TCRs (Fig. 5B). In 58 T cells, the differences in function of these TCR formats were not observed (Supporting Information Fig. 1). Moreover, the expression level of the different TCR formats on splenocytes directly correlated with small (not significant) differences in FRET efficiencies, which were more pronounced for the P14 TCR than for the OT-I TCR (Fig. 5C). These results demonstrate that the combination of TCR modifications improves correct TCR pairing on polyclonal T cells and that the level of improvement is TCR dependent.

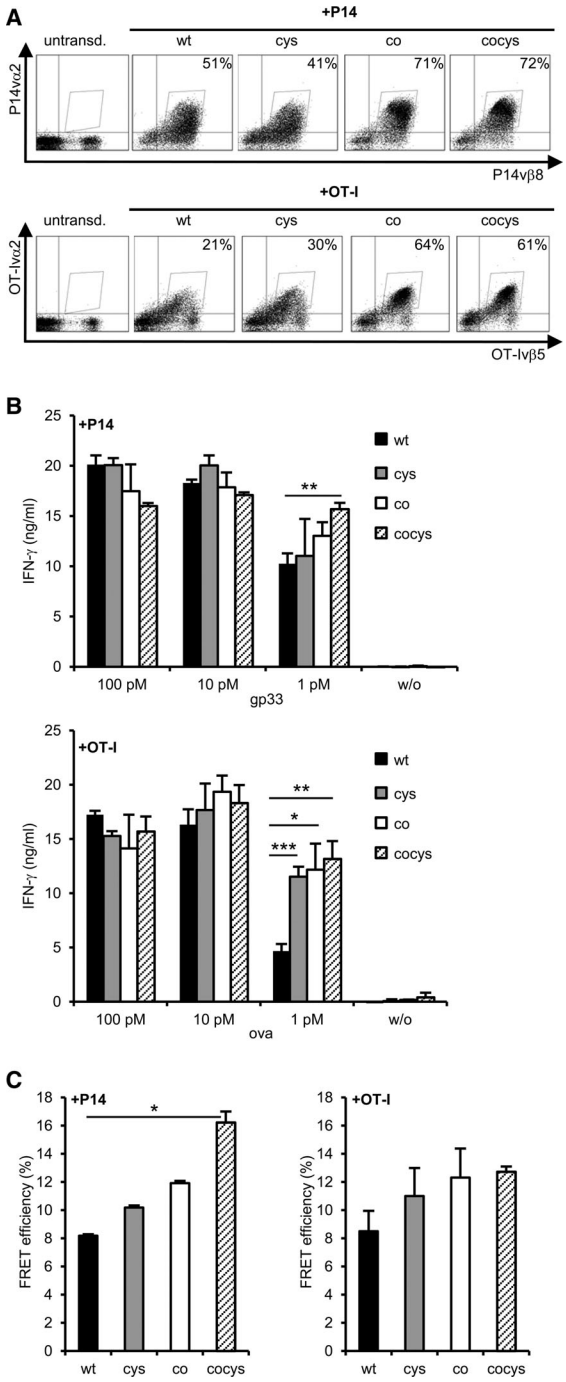

Figure 5. Primary C57BL/6 T cells transduced with different formats of P14 or OT-I TCRs. (A) C57BL/6 splenocytes were retrovirally transduced with different formats of the P14 (above) and OT-I TCR (below) and transduction rates were determined by TCR staining (P14: vβ8/vα2-Myc-Tag; OT-I: vβ5/vα2-HA-Tag). Live cells were discriminated in FSC/SSC dot plot. (B) IFN-γ secretion of primary C57BL/6 T cells transduced with the P14 (above) or OT-I TCR (below) after 24 h co-cultivation with peptide-loaded splenocytes. Bars indicate mean of triplets and mean deviation. (C) FRET efficiencies were calculated from staining as shown in (A). The mean and mean deviation of two separate measurements was determined. (A–C) Data shown are representative for one experiment out of three performed. $^{*}p < 0.05$; $^{**}p < 0.01$; $^{***}p < 0.001$; unpaired Student's *t*-test. cys: cysteineized-TCR with second cysteine bridge; co: codon-optimized TCR; cocys: codonoptimized and cysteineized TCR.

Discussion

In this study, we generated dual TCR T cells for a detailed analysis of the interaction between two TCRs under defined conditions. The expression level of the transduced TCRs was regulated either by using the constitutive promoter of the long terminal repeat of the retroviral vector LXSN [22] or the all-in-one vector Tet-on system [20] that offers the advantage to express all components of the Tet system from a single retroviral vector, with a good signal-to-noise ratio. Using the Tet-on vector system, we showed that the expression of both TCRs was inducible. To achieve a high TCR expression level, we used a Dox concentration of 1 μg/mL. For a low TCR expression level, we used 0.05 μg/mL Dox resulting in 50–60% TCR-positive cells. Lower Dox concentrations yielded a very low TCR expression (10–15%) and were considered as not suitable for our dual TCR expression analysis.

After induced TCR expression, we found that the constitutively expressed TCR remained on the cell surface but in lower numbers leading to a complete (P14 TCR) or partial (OT-I TCR) loss of function. That the expression of one TCR in dual TCR T cells can be reduced or lost was reported previously [23–26]. Another reason for this hampered function is the formation of mispaired TCR dimers. The occurrence of TCR mispairing was shown indirectly by not correlating TCRvβ chain and multimer staining in TCR-transduced T cells [9, 11, 27, 28]. In our study, multimer staining of the 58 cells (+CD8α) was not possible. In one report, FRET analysis was applied to quantify the improved pairing after the introduction of the CD3ζ into the TCR sequence [11]. In another study, TCR chain pairing measured by FRET was compared in HeLa and Jurkat cells [29]. This study is hampered by the fact that HeLa cells lack CD3 components, which have an impact on TCR pairing [30].

We also investigated correct pairing and mispairing of TCRα and β chains in dual TCR T cells by FRET. Besides correctly paired P14 and OT-I TCRs, we determined considerable occurrence of mispaired TCR dimers that was confirmed by the transfer of either the Tet-inducible TCR OT-Ivα2 or OT-Ivβ5 chain into P14 TCR-Tg 58 T cells. Additionally, we observed that especially the P14vβ8 chain and OT-Ivα2 chain are prone to form mispaired TCR dimers having a strong negative influence on correct P14 TCR pairing as well as on the TCR expression level of involved TCR chains. This may be due to still unknown intrinsic TCR properties and indicates that the degree of TCR mispairing depends on the individual TCR chain [30, 31]. In addition to reduced or even unequal TCR surface expression levels, TCR mispairing contributed to the loss of function of both TCRs in gene-modified T cells.

Two recent reports indicate that the formation of mispaired TCR dimers can lead to autoimmunity [5, 6]. In these cases, the introduction of a second cysteine bridge in the C-region of the Tg TCR led to a reduction of harmful reactivity. In order to evaluate the potential benefit of cysteineization for correct TCR chain pairing in our model, we introduced this modification in the P14 TCR gene, since this TCR was most prone to a reduction in FRET efficiency after induced OT-I TCR expression. In 58 T cells, we

could not rescue the function of the P14 TCR by cysteineization indicating that this modification alone is not sufficient to prevent mispairing in this cell model. However in polyclonal T cells, we detected little improvement in pairing of cysteineized and codon-optimized P14 and OT-I TCR. A higher degree of correctly paired TCRs resulted also in improved sensitivity of T-cell responses as measured by IFN-γ release at low Ag concentrations. These results are in agreement with previous reports showing on one hand that codon optimization leads to a higher translation rate of the Tg TCR, which then outpaces the endogenous TCR in the competition for limited amounts of CD3 proteins. On the other hand, the introduction of a second cysteine bridge in the TCR C-region facilitates the correct pairing of the Tg TCR chains and supports also efficient binding to the CD3 complex [13, 14].

In sum, our results demonstrate that cysteineization of TCR genes is not sufficient to completely avoid the formation of mispaired TCR dimers. Thus, other methods, which are recently under development, to avoid the expression of endogenous TCRs [32–34] should be used in the generation of TCR-Tg T cells for TCR gene therapy.

Materials and methods

Cell lines and primary cells

The ecotropic packaging cell line PlatE [35] was grown in DMEM (Gibco, Karlsruhe, Germany) with 10% FCS (Biochrom AG, Berlin, Germany), 100 units/mL penicillin/streptomycin (Gibco), and selective antibiotics (10 μg/mL blasticidin and 1 μg/mL puromycin (Sigma-Aldrich, Taufkirchen, Germany)). The 58 murine T-cell line [21] was grown in RPMI 1640+GlutaMax1 medium (Gibco) with 10% heat-inactivated FCS (PAN Biotech, Aidenbach, Germany), 100 units/mL penicillin/streptomycin, and 10 mM HEPES (Sigma-Aldrich). Murine splenocytes were grown in RPMI 1640+GlutaMax1 medium with 10% FCS (PAN Biotech), 1 mM sodium pyruvate, 1% nonessential amino acids, 100 units/mL penicillin/streptomycin (all Gibco), 1 mM HEPES, and 50 μM β-mercaptoethanol (Sigma-Aldrich).

Construction of TCR retrovirus vectors

The P14 TCR (vα2 = AV2S4 and vβ8 = BV8S1 [36]) is specific for the lymphocytic choriomeningitis virus glycoprotein peptide $gp_{33–41}$ (gp33: KAVYNFATM) presented in an H2-D^b-restricted manner. P14 TCR gene cloning with two myc tags (EQKLISEEDLEQKLISEEDL) at the N-terminus of the P14vα2 chain was described [37]. The OT-I TCR (vα2 = AV2S2 and vβ5 = BV5S2) is specific for the H2-K^b-restricted $OVA_{257–264}$ peptide (OVA: SIINFEKL) [38, 39]. The HA tag (YPYDVPDYA) was added to the N-terminus of the OT-Ivα2 chain by PCR. The single TCR chains were introduced into the MP71 vector [22] via NotI and EcoRI restriction sites and afterwards cloned in the conformation of TCRvβ–P2A–TCRvα as described [8]. TCR gene cassettes were blunt end ligated into the LXSN retrovirus vector [22] using HpaI restriction site. For the construction of the Tet-regulated MLV-SIN vector [20], the TCR transgene cassettes were cloned into the SK-T2-lmg* exchanging lmg transgene in SK-T2-lmg* and then, pTet-T2-TCR was cloned into the MLV-SIN vector via XhoI and NotI restriction sites. A second cysteine bridge was introduced by changing amino acids 187 and 186 from a threonine into a cysteine in the P14 and OT-I TCRvα chain, respectively, and amino acids 199 and 197 from a serine into a cysteine in the P14 and OT-I TCRvβ chain, respectively, by using overlapping PCRs. All primer sequences are provided on demand and primers were purchased from Eurofins MWG Operon (Ebersberg, Germany). The codon-optimized P14 and OT-I TCR genes were kindly provided by Jehad Charo (Berlin, Germany) and Ton Schumacher (Amsterdam, Netherlands), respectively.

Generation of TCR-Tg T cells

The 58 T-cell line and splenocytes were retrovirally transduced as described [8]. For generation of Tet-regulated TCR-expressing T-cell clones (either P14 or OT-I TCR), cells were incubated with 1 μg/mL Dox (Sigma-Aldrich) for 24 h, stained with TCRvβ-specific mAb, and sorted as single cells into 96-well round bottom plates (Corning Costar, Munich, Germany) using BD FACSAria flow cytometer (BD Bioscience, Heidelberg, Germany). Growing T-cell clones were analyzed for inducible TCR expression. One chosen T-cell clone was retrovirally transduced with a second TCR and single cell sorted for the TCRvβ chain expressed by the LTCRSN vector.

After transduction of splenocytes from C57BL/6 mice (Charles River, Sulzfeld, Germany), cells were cultured at a density of 1×10^6/mL with 10 ng/mL human recombinant IL-15 (PeproTech, Hamburg, Germany). All procedures were conducted according to the institutional guidelines.

Flow cytometric analysis of TCR expression

For the induction of Tet-regulated TCR expression, T cells were seeded at a density of 4×10^5/mL into a 24-well tissue culture plate with indicated Dox concentrations 24 h before analysis. For TCR staining following mAbs were used: anti-vα2 allophycocyanin mAb (Caltag Laboratories, Karlsruhe, Germany) or CD3ε allophycocyanin mAb (BD Pharmingen) in single TCR T cells, anti-myc mAb (clone 9E10; purified from hybridoma supernatant ATCC CRL-1729) or anti-HA mAb (clone 12CA; Roche Diagnostics, Mannheim, Germany) for P14 or OT-I TCR, respectively, in dual TCR T cells and transduced splenocytes, goat anti-mouse IgG Cy5 Fab fragment (Jackson Immunoresearch, West Grove, USA) for Tag staining, anti-TCRvβ8 PE or anti-TCRvβ5 PE mAb (both BD Pharmingen) for P14 and OT-I TCR, respectively, in single, dual TCR T cells and transduced splenocytes. For splenocytes staining, F_c block CD16/CD32 (BD Pharmingen) was used in advance.

TCR chains were quantified using the Qifikit® (Dako, Eching, Germany), with primary mAbs for Tag of TCRvα chains (as above) or with biotin-labeled mAbs for TCRvβ chains (BD Pharmingen). Flow cytometric analysis was done with a FACSCalibur flow cytometer using CellQuest Pro software (both BD Bioscience). Data analysis was performed with FlowJo software (TreeStar, Ashland, USA).

Cytokine release assay

T cells and peptide-loaded murine splenocytes (irradiated with 30 gray), each 8×10^4, were co-cultured in a 96-well round bottom plate for 24 h at 37°C. Cell number of TCR-transduced splenocytes and 58 T cells (for supporting information) was adjusted according to the transduction rate. For 58 T-cell clones with Tet-regulated TCR expression, Dox was added to the co-culture. For maximal stimulation, 5 ng/mL PMA (Sigma-Aldrich) and 1 μM ionomycin (Merck, Darmstadt, Germany) were added. Harvested supernatants were analyzed for secreted mouse IL-2 (eBioscience, San Diego, USA) of 58 T cells or for mouse IFN-γ (BD Bioscience) of splenocytes using ELISA according to the manufacturer's protocol. HPLC-purified peptides ($gp_{33–41}$: KAVYNFATM and $OVA_{257–264}$: SIINFEKL) were purchased from Biosynthan, Berlin, Germany.

Flow cytometry based FRET analysis

For FRET analysis, fluorescence intensities were measured using a FACSCalibur dual-laser flow cytometer (BD Biosciences). Emissions at 570 nm (donor channel, excitation at 488 nm), 670 nm (acceptor channel, excitation at 635 nm), and over 670 nm (FRET channel, excitation at 488 nm) were collected [11]. Data were analyzed with the aFLEX software on a per cell basis [40].

Statistical analysis

Unpaired Student's *t*-test was used to test statistical significance between different groups with $\alpha = 0.05$. *p*-Values were indicated for significance with asterisks $*p < 0.05$, $**p < 0.01$, and $***p < 0.001$. Measurements of duplicates were given as mean and mean deviation. Measurements of multiple experiments or triplets were given as mean ± SD.

Acknowledgments: We thank M. Richter, M. Kalupa, K. Hummel, and J. Hauchwitz for excellent technical support. For helpful discussions we thank T. Blankenstein, M. Leisegang, and M. Bunse. This work was supported by grants of the German Research Council (Grants SFB-TR36 and SPP1230 to W.U.) and the Helmholtz Society (Alliance on Immunotherapy of Cancer, Grant HA-202 to W.U.).

Conflict of interest: The authors declare no financial or commercial conflict of interest.

References

1 **Robbins, P. F., Morgan, R. A., Feldman, S. A., Yang, J. C., Sherry, R. M., Dudley, M. E., Wunderlich, J. R. et al.**, Tumor regression in patients with metastatic synovial cell sarcoma and melanoma using genetically engineered lymphocytes reactive with NY-ESO-1. *J. Clin. Oncol.* 2011. **29**: 917–924.

2 **Morgan, R. A., Dudley, M. E., Wunderlich, J. R., Hughes, M. S., Yang, J. C., Sherry, R. M., Royal, R. E. et al.**, Cancer regression in patients after transfer of genetically engineered lymphocytes. *Science* 2006. **314**: 126–129.

3 **Johnson, L. A., Morgan, R. A., Dudley, M. E., Cassard, L., Yang, J. C., Hughes, M. S., Kammula, U. S. et al.**, Gene therapy with human and mouse T-cell receptors mediates cancer regression and targets normal tissues expressing cognate antigen. *Blood* 2009. **114**: 535–546.

4 **Parkhurst, M. R., Yang, J. C., Langan, R. C., Dudley, M. E., Nathan, D.-A. N., Feldman, S. A., Davis, J. L. et al.**, T cells targeting carcinoembryonic antigen can mediate regression of metastatic colorectal cancer but induce severe transient colitis. *Mol. Ther.* 2011. **19**: 620–626.

5 **Bendle, G. M., Linnemann, C., Hooijkaas, A. I., Bies, L., de Witte, M. A., Jorritsma, A., Kaiser, A. D. M. et al.**, Lethal graft-versus-host disease in mouse models of T cell receptor gene therapy. *Nat. Med.* 2010. **16**: 565–570.

6 **van Loenen, M. M., de Boer, R., Amir, A. L., Hagedoorn, R. S., Volbeda, G. L., Willemze, R., van Rood, J. J. et al.**, Mixed T cell receptor dimers harbor potentially harmful neoreactivity. *Proc. Natl. Acad. Sci. USA* 2010. **107**: 10972–10977.

7 **Scholten, K. B. J., Kramer, D., Kueter, E. W. M., Graf, M., Schoedl, T., Meijer, C. J. L. M., Schreurs, M. W. J. et al.**, Codon modification of T cell receptors allows enhanced functional expression in transgenic human T cells. *Clin. Immunol.* 2006. **119**: 135–145.

8 **Leisegang, M., Engels, B., Meyerhuber, P., Kieback, E., Sommermeyer, D., Xue, S.-A., Reuß, S. et al.**, Enhanced functionality of T cell receptor-redirected T cells is defined by the transgene cassette. *J. Mol. Med.* 2008. **86**: 573–583.

9 **Xue, S.-A., Gao, L., Thomas, S., Hart, D. P., Xue, J. Z., Gillmore, R., Voss, R.-H. et al.**, Development of a Wilms' tumor antigen-specific T-cell receptor for clinical trials: engineered patient's T cells can eliminate autologous leukemia blasts in NOD/SCID mice. *Haematologica* 2010. **95**: 126–134.

10 **Willemsen, R. A., Weijtens, M. E., Ronteltap, C., Eshhar, Z., Gratama, J. W., Chames, P. and Bolhuis, R.**, Grafting primary human T lymphocytes with cancer-specific chimeric single chain and two chain TCR. *Gene Ther.* 2000. **7**: 1369–1377.

11 **Sebestyén, Z., Schooten, E., Sals, T., Zaldivar, I., San José, E., Alarcón, B., Bobisse, S. et al.**, Human TCR that incorporate CD3ζ induce highly preferred pairing between TCRα and β chains following gene transfer. *J. Immunol.* 2008. **180**: 7736–7746.

12 **Cohen, C. J., Zhao, Y., Zheng, Z., Rosenberg, S. A. and Morgan, R. A.**, Enhanced antitumor activity of murine-human hybrid T-cell receptor (TCR) in human lymphocytes is associated with improved pairing and TCR/CD3 stability. *Cancer Res.* 2006. **66**: 8878–8886.

13 **Kuball, J., Dossett, M. L., Wolfl, M., Ho, W. Y., Voss, R.-H., Fowler, C. and Greenberg, P. D.**, Facilitating matched pairing and expression of TCR chains introduced into human T cells. *Blood* 2007. **109**: 2331–2338.

14 **Cohen, C. J., Li, Y. F., El-Gamil, M., Robbins, P. F., Rosenberg, S. A. and Morgan, R. A.**, Enhanced antitumor activity of T cells engineered to express T-cell receptors with a second disulfide bond. *Cancer Res.* 2007. **67**: 3898–3903.

15 **Voss, R.-H., Willemsen, R. A., Kuball, J., Grabowski, M., Engel, R., Intan, R. S., Guillaume, P. et al.**, Molecular design of the Cαβ interface favors specific pairing of introduced TCRαβ in human T cells. *J. Immunol.* 2008. **180**: 391–401.

16 **Aggen, D. H., Chervin, A. S., Schmitt, T. M., Engels, B., Stone, J. D., Richman, S. A., Piepenbrink, K. H. et al.**, Single-chain V[alpha]V[beta] T-cell receptors function without mispairing with endogenous TCR chains. *Gene Ther.* 2012. **19**: 365–374.

17 **Govers, C., Sebestyén, Z., Coccoris, M., Willemsen, R. A. and Debets, R.**, T cell receptor gene therapy: strategies for optimizing transgenic TCR pairing. *Trends Mol. Med.* 2010. **16**: 77–87.

18 **Bialer, G., Horovitz-Fried, M., Ya'acobi, S., Morgan, R. A. and Cohen, C. J.**, Selected murine residues endow human TCR with enhanced tumor recognition. *J. Immunol.* 2010. **184**: 6232–6241.

19 **Sommermeyer, D. and Uckert, W.**, Minimal amino acid exchange in human TCR constant regions fosters improved function of TCR gene-modified T cells. *J. Immunol.* 2010. **184**: 6223–6231.

20 **Heinz, N., Schambach, A., Galla, M., Maetzig, T., Baum, C., Loew, R. and Schiedlmeier, B.**, Retroviral and transposon-based Tet-regulated all-in-one vectors with reduced background expression and improved dynamic range. *Hum. Gene Ther.* 2011. **22**: 166–176.

21 **Letourneur, F. and Malissen, B.**, Derivation of a T cell hybridoma variant deprived of functional T cell receptor α and β chain transcripts reveals a nonfunctional α-mRNA of BW5147 origin. *Eur. J. Immunol.* 1989. **19**: 2269–2274.

22 **Engels, B., Cam, H., Schüler, T., Indraccolo, S., Gladow, M., Baum, C., Blankenstein, T. et al.**, Retroviral vectors for high-level transgene expression in T lymphocytes. *Hum. Gene Ther.* 2003. **14**: 1155–1168.

23 **Sommermeyer, D., Neudorfer, J., Weinhold, M., Leisegang, M., Engels, B., Noessner, E., Heemskerk, M. H. M. et al.**, Designer T cells by T cell receptor replacement. *Eur. J. Immunol.* 2006. **36**: 3052–3059.

24 **Fossati, G., Cooke, A., Papafio, R. Q., Haskins, K. and Stockinger, B.**, Triggering a second T cell receptor on diabetogenic T cells can prevent induction of diabetes. *J. Exp. Med.* 1999. **190**: 577–584.

25 **Gladow, M., Uckert, W. and Blankenstein, T.**, Dual T cell receptor T cells with two defined specificities mediate tumor suppression via both receptors. *Eur. J. Immunol.* 2004. **34**: 1882–1891.

26 **Weinhold, M., Sommermeyer, D., Uckert, W. and Blankenstein, T.**, Dual T cell receptor expressing CD8+ T cells with tumor- and self-specificity can inhibit tumor growth without causing severe autoimmunity. *J. Immunol.* 2007. **179**: 5534–5542.

27 **Jorritsma, A., Gomez-Eerland, R., Dokter, M., van de Kasteele, W., Zoet, Y. M., Doxiadis, I. I. N., Rufer, N. et al.**, Selecting highly affine and well-expressed TCRs for gene therapy of melanoma. *Blood* 2007. **110**: 3564–3572.

28 **Abad, J. D., Wrzensinski, C., Overwijk, W., De Witte, M. A., Jorritsma, A., Hsu, C., Gattinoni, L. et al.**, T-cell receptor gene therapy of established tumors in a murine melanoma model. *J. Immunother.* 2008. **31**: 1–6. doi: 10.1097/CJI.1090b1013e31815c31193f.

29 **Shao, H., Zhang, W., Hu, Q., Wu, F., Shen, H. and Huang, S.**, TCR mispairing in genetically modified T cells was detected by fluorescence resonance energy transfer. *Mol. Biol. Rep.* 2010. **37**: 3951–3956.

30 **Heemskerk, M. H. M., Hagedoorn, R. S., van der Hoorn, M. A. W. G., van der Veken, L. T., Hoogeboom, M., Kester, M. G. D., Willemze, R. et al.**, Efficiency of T-cell receptor expression in dual-specific T cells is controlled by the intrinsic qualities of the TCR chains within the TCR-CD3 complex. *Blood* 2007. **109**: 235–243.

31 **Thomas, S., Xue, S.-A., Cesco-Gaspere, M., San José, E., Hart, D. P., Wong, V., Debets, R. et al.**, Targeting the Wilms tumor antigen 1 by TCR gene transfer: TCR variants improve tetramer binding but not the function of gene modified human T cells. *J. Immunol.* 2007. **179**: 5803–5810.

32 **Okamoto, S., Mineno, J., Ikeda, H., Fujiwara, H., Yasukawa, M., Shiku, H. and Kato, I.**, Improved expression and reactivity of transduced tumor-specific TCRs in human lymphocytes by specific silencing of endogenous TCR. *Cancer Res.* 2009. **69**: 9003–9011.

33 **Ochi, T., Fujiwara, H., Okamoto, S., An, J., Nagai, K., Shirakata, T., Mineno, J. et al.**, Novel adoptive T-cell immunotherapy using a WT1-specific TCR vector encoding silencers for endogenous TCRs shows marked anti-leukemia reactivity and safety. *Blood* 2011. **118**: 1495–1503.

34 **Provasi, E., Genovese, P., Lombardo, A., Magnani, Z., Liu, P.-Q., Reik, A., Chu, V. et al.**, Editing T cell specificity towards leukemia by zinc finger nucleases and lentiviral gene transfer. *Nat. Med.* 2012. **18**: 807–815.

35 **Morita S., Kojima T. and Kitamura, T.**, Plat-E: an efficient and stable system for transient packaging of retroviruses. *Gene Ther.* 2000. **7**: 1063–1066.

36 **Arden, B., Clark, S. P., Kabelitz, D. and Mak, T. W.**, Mouse T-cell receptor variable gene segment families. *Immunogenetics* 1995. **42**: 501–530.

37 **Kieback, E., Charo, J., Sommermeyer, D., Blankenstein, T. and Uckert, W.**, A safeguard eliminates T cell receptor gene-modified autoreactive T cells after adoptive transfer. *Proc. Natl. Acad. Sci. USA* 2008. **105**: 623–628.

38 **Schüler, T. and Blankenstein, T.**, Cutting edge: CD8+ effector T cells reject tumors by direct antigen recognition but indirect action on host cells. *J. Immunol.* 2003. **170**: 4427–4431.

39 **Hogquist, K. A., Jameson, S. C., Heath, W. R., Howard, J. L., Bevan, M. J. and Carbone, F. R.**, T cell receptor antagonist peptides induce positive selection. *Cell* 1994. **76**: 17–27.

40 **Szentesi, G., Horváth, G., Bori, I., Vámosi, G., Szöllősi, J., Gáspár, R., Damjanovich, S. et al.**, Computer program for determining fluorescence resonance energy transfer efficiency from flow cytometric data on a cell-by-cell basis. *Comput. Methods Programs Biomed.* 2004. **75**: 201–211.

Abbreviations: **C**: constant · **co**: codon-optimized TCR · **cocys**: codon-optimized and cysteineized TCR · **con**: constitutive expression · **cys**: cysteineized-TCR with second cysteine bridge · **Dox**: doxycycline · **FRET**: fluorescence resonance energy transfer · **ind**: induced expression · **Tet**: tetracycline (in this case, doxycycline)

Full correspondence: Dr. Wolfgang Uckert, Max Delbrück Center for Molecular Medicine, Robert-Rössle-Strasse 10, D-13092 Berlin, Germany
Fax: +49 (0) 30 9406 3306
e-mail: wuckert@mdc-berlin.de

Current address: Zsolt Sebestyén, Department of Hematology, University Medical Center Utrecht, Utrecht, Netherlands

Received: 3/4/2013
Revised: 1/8/2013
Accepted: 12/9/2013
Accepted article online: 30/9/2013